Discretization methods of the breakup continuum in deuteron-nucleus collisions

Rene Y. Rasoanaivo* and George H. Rawitscher
Department of Physics, University of Connecticut, Storrs, Connecticut 06268
(Received 28 November 1988)

Two methods of discretization of the *s*-wave *n-p* breakup continuum are compared, and their effect on the elastic deuteron-nucleus scattering matrix elements is numerically investigated. In one of the methods, the continuum eigenstates of the *n-p* Hamiltonian are averaged over discretized momentum bins of size Δk. In the other, which is a form of the L^2 diagonalization method, the continuum is expanded in a set of normalizable basis functions, which physically correspond to placing the *n-p* potential into a box. It is found, in the case of ^{58}Ni(*d*,*d*) at incident deuteron energies $E_d = 2.16$ and 45 MeV, that those two discretization techniques consistently display the same physics and yield the same results. However, the lower the incident deuteron energy, the less well do the momentum discretized answers converge to a final result. The diagonalization method is found to perform better in this respect. The theoretical expectation that the long range tails of the potentials in breakup space do not sensitively affect the elastic *S*-matrix elements is demonstrated numerically. This result provides the mathematical reason why the discretization of the breakup continuum is a viable and practical procedure of including the breakup effects.

I. INTRODUCTION

The effect which the breakup of the deuteron, in the nuclear field, has on the elastic deuteron scattering is described by a set of integrodifferential equations which couple the elastic channel with a continuously infinite number of breakup channels. Because these equations cannot be solved by the usual numerical techniques, methods of discretization are required in order to reduce the coupled differential equations to a finite discrete set. Various types of discretization methods have already been discussed in the literature, and the present study addresses itself to two particular ones which have been used for the case of deuteron-nucleus scattering. One is the discretization of the momentum continuum into finite bins of size Δk,[1-5] which will be referred to as the *k*-bin method in this report, and the other is the diagonalization procedure[6-9] of the *n-p* Hamiltonian $H_{np}(\mathbf{r})$ in terms of L^2 functions. Both methods lead to a finite set of coupled equations now commonly denoted coupled discretized continuum channels (CDCC) which are different from Faddeev equations. The validity of these mathematical methods has been carefully analyzed in many respects. In particular, the investigation of the convergence of the *k*-bin discretization procedure was carried out by Kamimura and co-workers.[4] The same type of study for the L^2 method was also performed separately by Levin[8] and by Rasoanaivo.[9] The purpose of the present paper is to compare the two methods, i.e., to examine the sensitivity of the elastic scattering matrix elements $S(L)$ to the number and range of the discretization functions employed and inquire how the choice of the discretization method affects the convergence to the final result. Although our study of the *k*-bin discretization is not as extensive as Kamimura's, it still goes beyond in that it also discusses the diagonalization procedure and then compares the two methods. Furthermore, the basis functions which underly our diagonalization method are different from all the ones previously utilized.[6-8] Our basis functions are purposely designed so as to make the diagonalization more flexible for a close comparison.

Since the study, upon which this paper is based, was completed,[9] the validity of the CDCC method as a three-body model was questioned.[10] A study by Austern and Kawai[10] shows that the method has intrinsic validity in a limited region of channel space. This result is supported by Sawada and Thushima[10] who examine whether the opening of a stripping channel has a destabilizing effect on the CDCC breakup results. Within their limited size of the breakup channel space they do not find such an effect on the elastic and breakup *T* matrices, showing that the CDCC method is stable and unique. In view of this added justification for the CDCC procedure as a valid, albeit restricted (because it does not carry the rearrangement channels explicitly) three-body treatment, the present comparison between the L^2 method and the *k*-bin discretization method for solving the coupled equations mentioned above is of renewed interest. Initially the present study was motivated by the suspicion that the inclusion of the breakup effect on the elastic scattering or on the stripping cross sections might depend heavily on the treatment of the *n-p* continuum. In fact, the process of discretization inevitably introduces systematic errors into the calculations. For instance, the *k*-bin discretization method defines a maximum momentum $k_{\max}$ (which is the range of the momentum space to be discretized) and also the size, Δk, of the momentum bins. The quantity $k_{\max}$ is usually chosen such that only the open channels are included, since the closed channels carry no flux. However, the effect of the coupling between open and closed channels does not seem to be negligible in view of the large strength of the coupling potentials.[2] Therefore, for a given scattering energy, a different criterion for the choice of the maximum momentum $k_{\max}$ is desirable.

The same problem exists in the diagonalization procedure in which the eigenstates of the n-p Hamiltonian H_{np} are approximated by finite linear combinations of some L^2-functions. The size N of such expansions cannot be chosen *a priori* in a reliable manner. Given those various inherent problems of the CDCC, and given the fact that the use of CDCC has been extended to the analyses[11] of the breakup of light heavy ions like ^{6}Li, ^{7}Li, and ^{12}C, it seems reasonable to establish a close comparison of the two methods of discretization in the hope of clarifying what type of discretization is appropriate to a given reaction at some given energy.

II. THEORETICAL FORMALISM

The complete description of the CDCC approximation to the three-body system, $(n+p)+A$, has already been reported in several places.[12-13] Therefore, we restrict ourselves to the simplest form of the formulation and concentrate on the derivation of the coupled integrodifferential equations which is the main subject of the present report. Ignored are the stripping channels, the antisymmetrization, the spin, and the nonzero relative angular momenta. Furthermore, it is assumed that the interaction between the deuteron and target nucleus can be described by an effective complex optical potential $V_{\rm eff}(\mathbf{r},\mathbf{R})$ which is approximated by

$$V_{\rm eff}(\mathbf{r},\mathbf{R})=U_{p\text{-}A}\left(\left|\mathbf{R}-\frac{\mathbf{r}}{2}\right|\right)+U_{n\text{-}A}\left(\left|\mathbf{R}+\frac{\mathbf{r}}{2}\right|\right), \tag{2.1}$$

where $U_{p\text{-}A}$ and $U_{n\text{-}A}$ are, respectively, the proton nucleus optical potential and the neutron nucleus optical potential, both evaluated at an energy equal to half the incident deuteron energy E_d; $\mathbf{R}$ and $\mathbf{r}$ are, respectively, the deuteron c.m. position vector and the n-p relative position vector. The wave function of the scattering system then obeys the following "model" Schrödinger equation

$$[T(\mathbf{R})+H_{np}(\mathbf{r})+V_{\rm eff}(\mathbf{r},\mathbf{R})-E]\Psi(\mathbf{r},\mathbf{R})=0\ , \tag{2.2}$$

where $T(\mathbf{R})$ is the deuteron c.m. kinetic energy; $H_{np}(\mathbf{r})$ is the n-p relative Hamiltonian defined by $H_{np}(\mathbf{r})=T(\mathbf{r})+v_{np}(r)$. In the latter expression, $T(\mathbf{r})$ is the n-p relative kinetic energy and $v_{np}(r)$ the central n-p potential.

In order to separate the $\mathbf{r}$ dependence from that of the variable $\mathbf{R}$ one expands $\Psi(\mathbf{r},\mathbf{R})$ in terms of the eigenstates of $H_{np}(\mathbf{r})$

$$\Psi(\mathbf{r},\mathbf{R})=\phi_d(\mathbf{r})X_d(\mathbf{R})+\int\phi_k(\mathbf{r})X_k(\mathbf{R})d\mathbf{k}\ , \tag{2.3}$$

where $\phi_d(\mathbf{r})$ and $\phi_k(\mathbf{r})$ are, respectively, the deuteron bound and scattering states. The function $X_d(\mathbf{R})$ is the deuteron c.m. wave function and the functions $X_k(\mathbf{R})$ are the broken up deuteron c.m. wave functions which correspond to the breakup states defined by $\phi_k(\mathbf{r})$. The functions $X_k(\mathbf{R})$ are only outgoing waves at large distances R, while $X_d(\mathbf{R})$ contains both incoming and outgoing waves. If one now substitutes (2.3) into (2.2) and then multiplies the subsequent equation, respectively, by $\Phi_d(\mathbf{r})$ and $\Phi_k(\mathbf{r})$, and integrates each time with respect to the variable $\mathbf{r}$, one obtains the following coupled equations

$$[T(\mathbf{R})+\varepsilon_d-E]X_d(\mathbf{R})+V_{dd}(\mathbf{R})X_d(\mathbf{R})+\int d\mathbf{k}V_{dk}(\mathbf{R})X_k(\mathbf{R})=0\ , \tag{2.4a}$$

$$[T(\mathbf{R})+\varepsilon_k-E]X_k(\mathbf{R})+V_{kd}(\mathbf{R})X_d(\mathbf{R})+\int d\mathbf{k}V_{kk'}(\mathbf{R})X_{k'}(\mathbf{R})=0\ , \tag{2.4b}$$

where

$$V_{ij}(\mathbf{R})=\int\Phi_i(\mathbf{r})V_{\rm eff}(\mathbf{r},\mathbf{R})\Phi_j(\mathbf{r})d\mathbf{r} \tag{2.5}$$

with $i,j=d,\mathbf{k},\mathbf{k}'$. The above equations represent the coupling between an infinitely continuous set of functions (in the variable k) and, thus they cannot be solved exactly. The coupling potentials $V_{kd}(\mathbf{R})$ and $V_{kk'}(\mathbf{R})$ have nonnegligible strength and a long range in the variable R. In the k-bin method, the discretization technique consists in averaging the coupling potentials over momentum bins of size Δk and replacing the integrals over k by discrete sums, whereas in the L^2 diagonalization procedure the basis functions are chosen from the start as a discrete and complete set, as will be now discussed.

A. Diagonalization procedure

The basic idea[14] of the diagonalization procedure is to construct a set of orthogonal basis functions $\Phi(\mathbf{r})$ which minimize the quantity $J=\langle\Phi|H_{np}-\varepsilon|\Phi\rangle$. The trial functions $\Phi(\mathbf{r})$ are given by the finite expansion

$$\Phi^{(N)}(\mathbf{r})=\sum_{i=1}^{N}C_i\phi_i(\mathbf{r})\ , \tag{2.6}$$

where the functions $\phi_i(\mathbf{r})$ are L^2 functions such as negative-energy Weinberg functions,[6,7] local Gaussian functions,[1] or Laguerre functions.[9] The coefficient C_i, which are the variational parameters, are such that

$$\frac{\partial J}{\partial C_i}=0,\quad i=1,2,\ldots,N\ . \tag{2.7}$$

The condition above yields a system of homogeneous linear equations in the C_i's

$$\sum_{i=1}^{N}\langle\phi_j|H_{np}-\varepsilon|\phi_i\rangle C_i=0\ , \tag{2.8}$$

which admits nontrivial solutions only if the determinant vanishes

$$\det|\langle\phi_j|H_{np}-\varepsilon|\phi_i\rangle|=0\ . \tag{2.9}$$

The above equation is an eigenvalue problem which, in general, can be solved numerically without difficulty. For each eigenvalue ε_n, a set of coefficients C_n is found, with $n=1,2,\ldots,N$. The discretization is thus achieved through the process of truncating the set of basis functions to the finite number N.

In the present study, the functions $\phi_i(\mathbf{r})$ are generated by a harmonic oscillator potential $w(r)$ which is added to the n-p potential $v_{np}(r)$ (see Fig. 1):

$$[H_{np}+w(r)-\xi_i]\phi_i(\mathbf{r})=0\ , \tag{2.10}$$

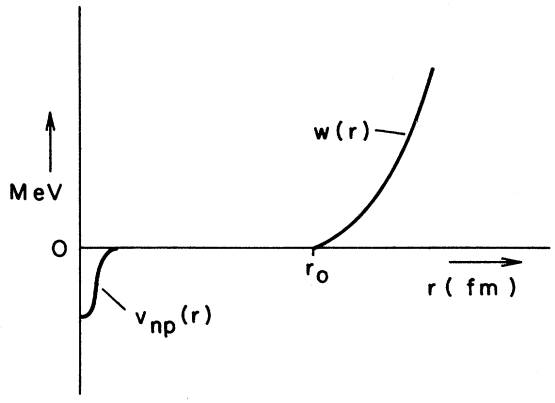

FIG. 1. Diagram of $v_{np}+w(r)$.

where $w(r)=\alpha(r-r_0)^2$ for $r>r_0$ and $w(r)=0$ for $r<r_0$. The $\phi_i(\mathbf{r})$'s are regular at the origin and asymptotically they go to zero. The parameters α and r_0 are real and can be chosen arbitrarily. If the distance r_0 is taken to be sufficiently greater than the range of the deuteron bound-state function $\Phi_d(\mathbf{r})$, then a single negative energy eigenfunction $\phi_1(\mathbf{r})$, which is very close to the deuteron bound-state function, is obtained. This will facilitate the numerical task of extracting the elastic component from the wave function.

The present choice of the L^2 basis functions provides some interesting advantages. First, unlike, the other diagonalization methods[6–8] which depend on a single parameter N, the present technique allows a systematic increase of the configuration space by just displacing the point r_0 without involving a great number of L^2 functions, which is unavoidable otherwise. Second, the method permits one to control separately the number of basis states per breakup energy interval.

The wave function is now expanded in the set of functions described above, but since only a finite number of them is used, the expansion is incomplete and a truncation error remains

$$\Psi(\mathbf{r},\mathbf{R})=\sum_{n=1}^{N}\Phi_n^{(N)}(\mathbf{r})X_n^{(N)}(\mathbf{R})+\text{ truncation error }. \tag{2.11}$$

B. The truncated coupled equations

The "discretized" coupled differential equations obtained by both the diagonalization and the k-bin methods can be written in the form

$$[T(\mathbf{R})-E+\varepsilon_n^{(N)}]X_n^{(N)}(\mathbf{R})+\sum_{n'}^{N'}V_{n,n'}^{(N)}(\mathbf{R})X_{n'}^{(N)}(\mathbf{R})=0\ , \tag{2.12}$$

and should be solved with the same boundary conditions as the original equations (2.4). In fact, the functions $X_n^{(N)}(\mathbf{R})$, which play the role of the functions $X_d(\mathbf{R})$ and $X_k(\mathbf{R})$, can be written as

$$X_n^{(N)}(\mathbf{R})=\frac{1}{R}\sum_{LM}F_{nL}^{(N)}(R)Y_{LM}(\hat{R})\ , \tag{2.13}$$

where the radial parts $F_{nL}(R)$ have the asymptotic form

$$F_{nL}^{(N)}(R)=\frac{1}{2i}[-H_L^{(-)}(K_n^{(N)}R)\delta_{1n}+S_n^{(N)}H_L^{(+)}(K_n^{(N)}R)]\ . \tag{2.14}$$

The function $H_L^{(-)}(K_n^{(N)}R)$ and $H_L^{(+)}(K_n^{(N)}R)$, respectively, represent the incoming and outgoing Coulomb waves. The quantity $S_n^{(N)}$ is the scattering matrix element in channel n, and L is the angular momentum of the center of mass of the n-p pair relative to the nucleus; the corresponding linear momentum is denoted by $K_n^{(N)}$ and given by

$$K_n^{(N)}=\left[\frac{2M}{\hbar^2}\right][(E_d)_{\text{c.m.}}+\varepsilon_d-\varepsilon_n^{(N)}]^{1/2}\ , \tag{2.15}$$

where $(E_d)_{\text{c.m.}}$ is the incident deuteron energy in the c.m. system. The total number of states used for the discretization procedure is denoted by N, and $n=1,2,3,\ldots,N$ denotes any one of the channels, including the elastic channel for which $n=1$. Furthermore, the coupling potentials $V_{nn'}^{(N)}(\mathbf{R})$ are defined by

$$V_{nn'}^{(N)}(\mathbf{R})=\int_0^\infty\Phi_n^{(N)}(\mathbf{r})V_{\text{eff}}(\mathbf{r},\mathbf{R})\Phi_{n'}^{(N)}d\mathbf{r}\ . \tag{2.16}$$

We notice that, since the functions $\Phi_n^{(N)}(\mathbf{r})$ are bound functions, which decay asymptotically to zero faster than exponentially, the above coupling potentials have shorter ranges than their counterparts in (2.5), which decrease like R^{-2} times an oscillatory function of R. It is assumed in this formalism that as N increases, which corresponds to Δk becoming small in the k-bin method, the truncation error in the expansion (2.11) will decrease, the range of those coupling potentials (2.16) will be restored and, because the breakup space being included becomes large, the scattering matrix $S_n^{(N)}(L)$ will converge to some fixed value. These expectations will be borne out in the context of the diagonalization procedure as will be seen in the following calculations.

III. NUMERICAL ANALYSIS

The two discretization procedures previously discussed are examined numerically for deuteron ^{58}Ni scattering at incident deuteron laboratory energies of 21.6 and 45 MeV. Each choice of a discretization method leads to different coupling potentials and a different number of channels, as is discussed in detail below. The resulting coupled equations, (2.12) are then solved with the Numerov method,[15,16] and the behavior of the elastic scattering matrix elements, in particular their convergence to a final value, is examined. The change in the discretization parameters also changes the long-range part of the radial dependence of the channel and coupling potentials for the breakup channels. A theoretical study[17] shows that changes in these potentials which occur beyond the range of the elastic to breakeup coupling potentials should not significantly affect the elastic

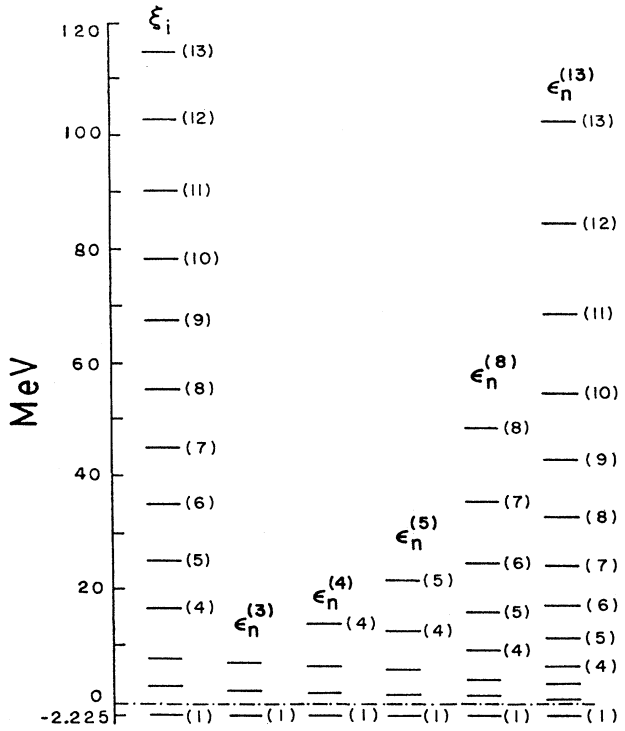

FIG. 2. The eigenvalues $\varepsilon_n^{(N)}$ of $H_{np}(\mathbf{r})$ for $r_0=12$ fm and $\alpha=0.52$ MeV/fm^2.

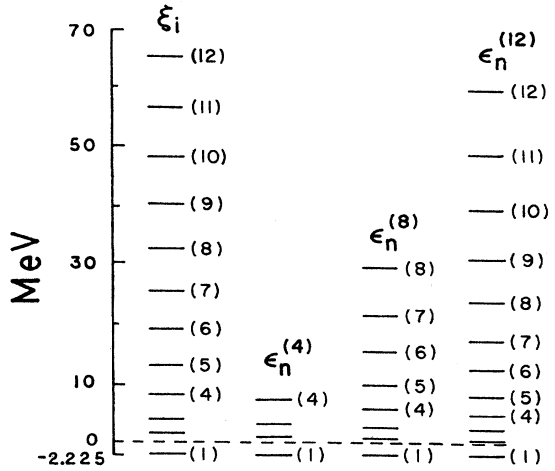

FIG. 3. Same as in Fig. 2 with the same value of α but with $r_0=20$ fm.

scattering matrix elements, and a numerical confirmation of this result is also provided further below.

A. The diagonalization method of discretization

In order to carry out the diagonalization procedure, a number N of bound functions $\phi_i(\mathbf{r})$ are first calculated for two values of r_0 (12 and 20 fm) and for $\alpha=0.52$ MeV/fm^2. The nucleon-nucleon potential has the form

$$v_{np}(r)=-V_0\exp(-\beta r^2)\,,\qquad V_0=66.92\text{ MeV},\quad \beta=0.415\text{ fm}^{-2}\,, \tag{3.1}$$

which is in agreement with previous work.[2] Next the Eqs. (2.8), (2.9), and (2.10) are solved numerically. That yields a set of N discrete eigenenergies $\varepsilon_n^{(N)}$. The corresponding eigenfunctions are obtained by simply substituting ϕ_i into Eq. (2.6). Figures 2 and 3 show the various eigenenergies obtained with different values of N. For a given choice of N, the coupling potentials (2.16) are calculated with nucleon-nucleus optical potential parameters taken from the works of Perey and Buck,[18] and also Becchetti and Greenlees,[19] following the procedure of Ref. 9. The parameters are listed in Table I. $V_{\text{eff}}(r,R)$ is given by the zero-order multipole of the potential defined in (2.1), as is further described in Ref. 9. Some of the potentials are illustrated in Figs. 4 and 5. For each choice of N the number of channels n included in the solution of the coupled equations is increased successively from one (in this case there is no coupling to breakup channels) to its maximum value N, and the corresponding elastic scattering matrix elements $S_1^N(L)$ are plotted as a function of n. Some of the results are illustrated in Figs. 6–9, where n is denoted as $n-1$. Thus, the results obtained

TABLE I. Nucleon-nucleus optical potential parameters corresponding to nucleon energies equal to half incident deuteron energy E_d.

E_d (MeV)	21.6[a]		45[a]		80[b]	
Nucleon	n	p	n	p	n	p
V_V (MeV)	−49.56	−51.60	−48.272	−50.52	−42.67	−44.92
r_V (fm)	5.28	5.00	4.528	4.528	4.52	4.52
a_V (fm)	0.62	0.65	0.75	0.75	0.75	0.75
V_I (MeV)	0.00	0.00	−3.35	−2.25	−7.20	−6.10
r_I (fm)	5.00	5.00	4.87	5.109	4.877	5.11
a_I (fm)	0.60	0.60	0.58	0.53	0.58	5.3
W_D (fm)	−3.57	−13.16	−6.961	−6.58	−2.58	−2.21
r_D (fm)	5.28	5.00	4.87	5.10	4.87	5.11
a_D (fm)	0.65	0.57	0.58	0.53	0.58	0.53

[a]From Ref. 18.
[b]From Ref. 19.

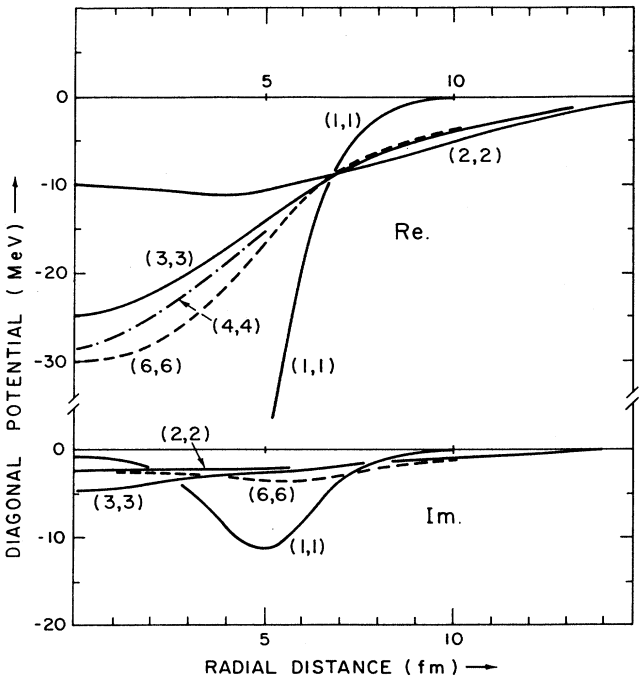

FIG. 4. Diagonal distorting potentials in channels 1–6, obtained for the diagonalization procedure of discretization with the parameters r_0 and α equal to 20 fm and 0.52 MeV fm^{-2}, respectively. Channel 1 is the elastic deuteron channel. The Coulomb potentials are not yet included.

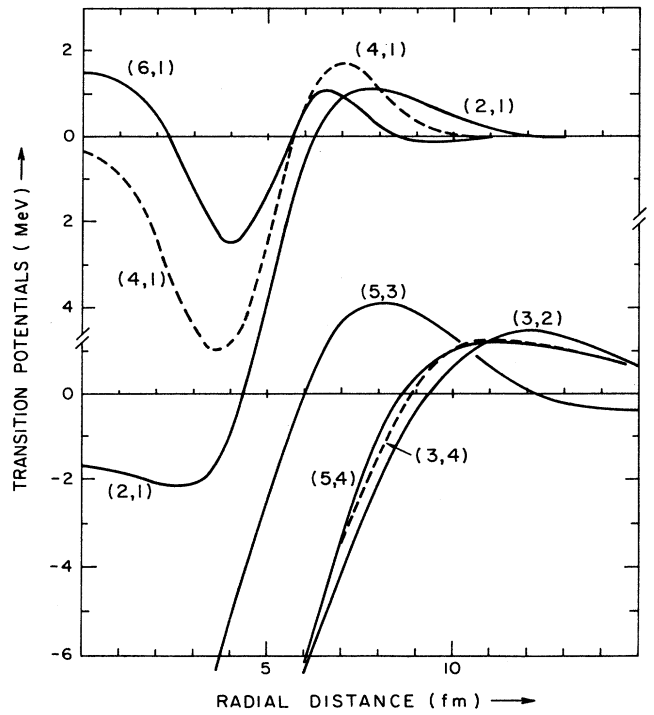

FIG. 5. Real parts of some interchannel coupling potentials for the conditions described in Fig. 3. The upper part shows elastic to breakup transition potentials, the lower part shows breakup to breakup transition potentials. The range of the latter is visibly larger than the range of the former.

without coupling to any breakup channels are shown for $n=0$. The results for the absolute values of $S_1^{(N)}(L)$ the reflection coefficients, are shown in Figs. 6 and 7 for $E_d=21.6$ MeV and for $r_0=20$ fm. Figures 8 and 9 show the results for $E_d=45$ MeV, in which the two sets of $\Phi_n^{(N)}(\mathbf{r})$'s correspond to $N=8$ and 13, and $r_0=12$ fm. The values of the angular momenta L are written on the plots. We notice that as n increases the reflection coefficients first change randomly and, as n becomes large, converge to some stationary value. This convergence tends to be faster generally for high angular momenta than for low angular momenta. This feature is probably due to the fact that breakup channels associated to high breakup energies and thus to low channel energies $E_n^{(N)}=E-\varepsilon_n^{(N)}$ are being suppressed by the angular momentum barrier $L(L+1)/R^2$ when L gets large. Therefore, they carry little flux out of the elastic channel.

Moreover, it appears that all channels need not be included in order to reach convergence. In fact, what determines the number of channels n needed to obtain convergence, is to a large extent determined by the maximum value of the eigenenergy. For example, at

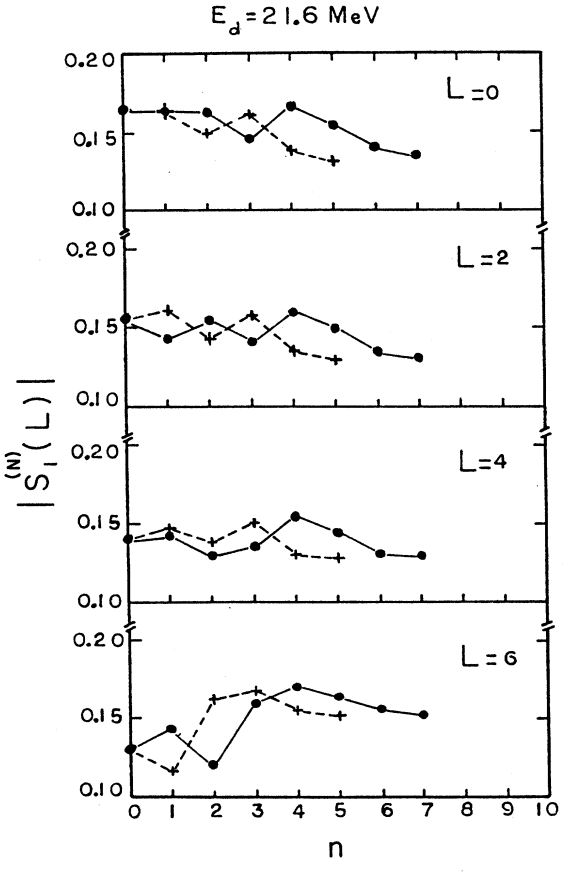

FIG. 6. Reflection coefficients $|S(L)|$ vs the number n of breakup couplings for even angular momenta L and $E_d=21.6$ MeV. The (+) denote results for a size of discretization space N of 12, and the (·) correspond to $N=8$. The value of r_0 is 20 fm.

$E_d=21.6$ MeV, for $N=8$ and 12 the corresponding convergence values of n are 5 and 6, respectively, and the corresponding eigenenergies are given by $\varepsilon_6^{(8)}=15.36$ MeV and $\varepsilon_7^{(12)}=17.65$ MeV. This is true for all L values between 0 and 13. Similarly, for $E_d=45$ MeV and a smaller value of r_0, the converged values of $|S_1^{(N)}|$ are obtained at slightly higher energies $\varepsilon_6^{(8)}=24.83$ MeV and $\varepsilon_7^{(13)}=24.21$ MeV for L between 0 and 15. It would be reasonable but misleading to expect that the maximum value of the eigenenergy $\varepsilon_n^{(N)}$ is determined by the conditions that the corresponding channel energy $E_n^{(N)}$ be negative, since no breakup flux is carried away by closed channels. This expectation is supported by the finding that for $E_d=21.6$ MeV the channels which could be neglected corresponded to negative values $E_n^{(N)}$. However, for $E_d=45$ MeV the channels which could be neglected started with $\varepsilon_8^{(13)}=32$ MeV, for which $E_n^{(N)}$ is still positive. Additional results can be found in Ref. 9.

The next question to be examined concerns the size N of the space of the basis set used to diagonalize the n-p Hamiltonian $H_{np}(\mathbf{r})$. For this purpose we examine the convergence of the reflection coefficients $|S_1^{(N)}(L)|$ this time with respect to the number N of the diagonalizing eigenstates. We proceed with various sets of the eigenfunctions $\Phi_n^{(N)}(\mathbf{r})$ obtained with $N=3$, 4, 5, 8, 12, and 13 and for each N we include as many channels n as are needed to obtain convergence for the S matrix elements. As suggested by the previous results, the calculations only involve open channels for both energies $E_d=21.6$ and $=45$ MeV. The converged values of $|S_1^{(N)}|$ obtained with each set of the functions $\Phi_n^{(N)}(\mathbf{r})$, for small partial waves ($L<10$), are plotted against N in Figs. 10 and 11 for both energies. The dashed lines interpolate the points which have not been calculated. We notice that for both energy cases convergence of $|S_1^{(N)}(L)|$ sets in at $N=5$. The breakup states for $N=5$ cover the breakup energy range of approximately 20 MeV. The fact that a lower incident deuteron energy requires the participation of a large range of breakup channels and energies indicates that the present method of including the effect of breakup may not be practical for very low incident deuteron energies. It also suggests a possible shortcoming of the adiabatic method which assumes that only the low n-p breakup energies ($\varepsilon_k<10$ MeV) are important. Furthermore, for the energy case $E_d=21.6$ MeV the points show some instability as N increases from 5 to 12 especially for the very low partial waves; on the other hand, for the case of $E_d=45$ MeV this instability is less pronounced. This result shows the sensitivity of the method of discretization to the choice of discretization parameters at the low

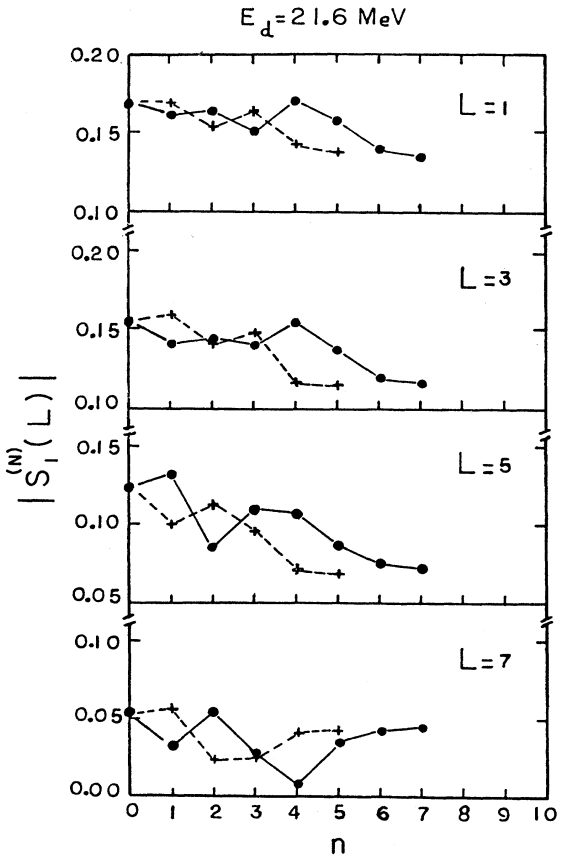

FIG. 7. Same as Fig. 6 for odd angular momenta L.

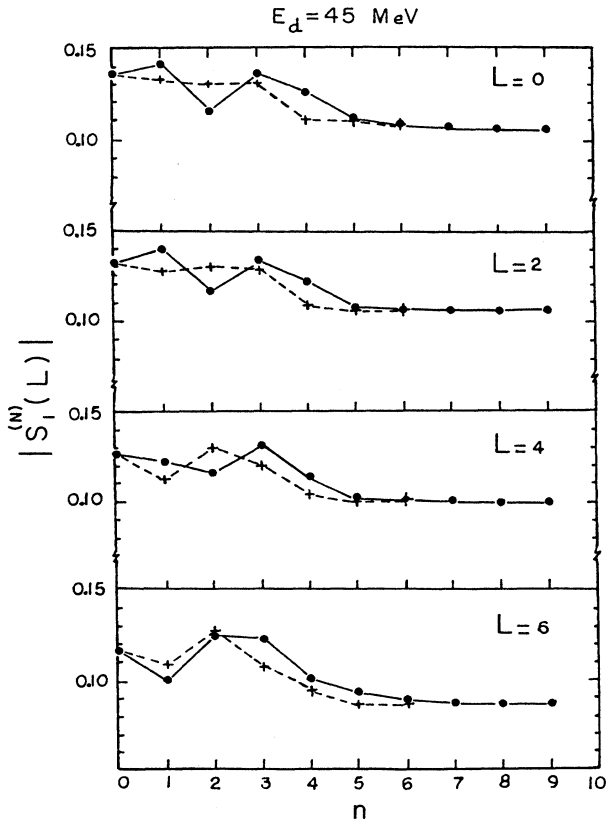

FIG. 8. Reflection coefficients $|S(L)|$ vs the number n of breakup couplings for even angular momenta L and $E_d=45$ MeV. The (+) and (-) correspond to $N=8$ and 13, respectively. $r_0=12$ fm.

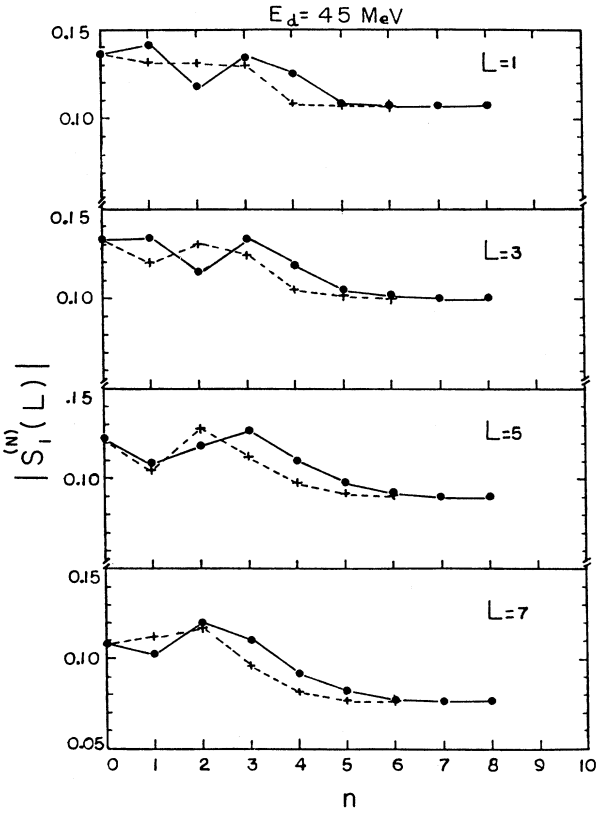

FIG. 9. Same as Fig. 8 for odd values of L.

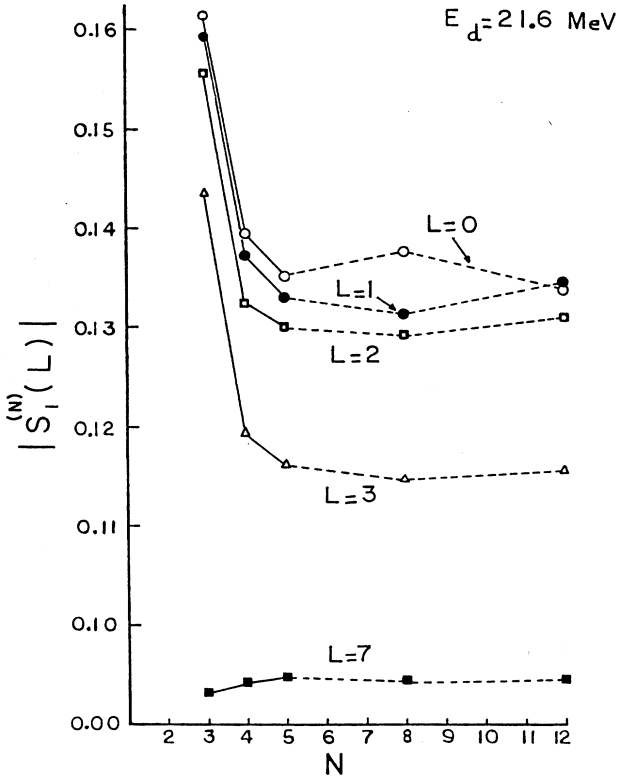

FIG. 10. Reflection coefficients $|S(L)|$ vs N, the number of diagonalized states, for small angular momenta and $E_d = 21.6$ MeV.

scattering energies. From Figs. 10 and 11 one can see that the amount of absorption of deuterons in the elastic channel increases ($|S|$ decreases) as the number of discretization channels increases. Hence a calculation of elastic or rearrangement cross sections which includes less than 20 MeV of breakup space is likely to be suspect.

B. The k-bin method of discretization

The purpose of the following calculations is to check the consistency of the discretization techniques through a comparison of the methods of diagonalization and bin discretization. The procedure developed by Rawitscher[2] is adopted here for the bin discretization calculation. This method is slightly different from the bin discretization procedure developed by Austern and co-workers.[3] We divide the n-p momentum space into bins of equal sizes Δk and for each bin we calculate the averaged transition potentials $\hat{V}_{ii'}(\mathbf{R})$ and the corresponding averaged n-p energies $\hat{\varepsilon}_i$ according to the definitions given in Ref. (2). These calculations are performed for various bin sizes $\Delta k = 0.48$, 0.24, and 0.12 fm^{-1}.

There is a close relation between the diagonalization and bin discretization method because the discrete momenta $(2m\varepsilon_n^{(N)}/\hbar^2)^{1/2}$ obtained from the diagonalization method are found to be practically equidistant, and thus correspond to a particular bin size in the k-bin method. For example, the bin size $\Delta k = 0.12$ fm^{-1} corresponds

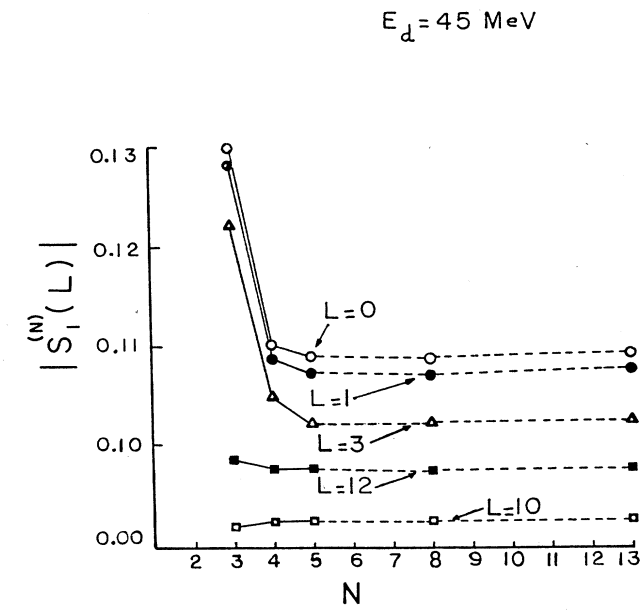

FIG. 11. Same as Fig. 10 for $E_d = 45$ MeV.

approximately to a diagonalization spectrum obtained for r_0 of 16 fm and $N=13$, or to r_0 of 20 fm and $N=8$. Similarly, $\Delta k=0.24$ fm^{-1} corresponds approximately to r_0 of 12 fm and $N=3$. In order to make a systematic comparison between the present diagonalization method and the k-bin method, we first study the convergence of the reflection coefficients $|\hat{S}(L)|$ with respect to the bin size Δk by using the k-bin method. Then, we compare the converged values of the elastic scattering matrix elements given by each method.

The calculations involve the same coupled differential equations derived previously. The transition potentials are computed with the same optical-potential parameters. The reflection coefficients $|\hat{S}(L)|$ for various angular momenta are plotted versus the number of the bins i in Figs. 12 and 13 for $E_d=21.6$ MeV, in Figs. 14 and 15 for $E_d=45$ MeV, and in Fig. 16 for $E_d=80$ MeV. Again, these calculations involve only open channels. In Figs. 12 and 13, the crosses indicate the results obtained with $\Delta k=0.48$ fm^{-1} in which case there is only one open channel corresponding to breakup energy $\hat{\varepsilon}_2=5$ MeV; the open circles refer to the results obtained with $\Delta k=0.24$ fm^{-1} with $\hat{\varepsilon}_5=18$ MeV, and the solid circles denote the results obtained with $\Delta k=0.12$ fm^{-1} with $\hat{\varepsilon}_5=15$ MeV.

We notice that there are large discrepancies between results obtained from $\Delta k=0.48$ fm^{-1} and those obtained from $\Delta k=0.24$ or 0.12 fm^{-1}; the latter two, however, seem to be in fairly good agreement with each other for every partial wave. In all of these calculations, the convergence of $|\hat{S}(L)|$ does not look as apparent as in the case of diagonalization calculations until the angular momenta get large, $L=11$ for instance. Even the points corresponding to small bins, $\Delta k=0.12$ fm^{-1}, do not show signs of convergence. This result confirms the argument made previously on the sensitivity to the discretization method at the low deuteron energies. At energies above 45 MeV the convergence of $|\hat{S}(L)|$ with bin size Δk becomes adequate, as is shown in Figs. 14 and 15, where solid circles designate results obtained with $\Delta k=0.24$ fm^{-1} and crosses correspond to $\Delta k=0.48$ fm^{-1}. The breakup space being covered is approximately the same in both cases; it is equal to 30 MeV for the first case ($\Delta k=0.24$ fm^{-1}) and to 26.5 MeV for the second case ($\Delta k=0.48$). Furthermore, for every partial wave, we notice that the crosses are pointing toward the converged values of the solid circles, and the distances between those two points diminish as L augments. In fact, for $L=9$ and 10, we find the same results for both bins. In the case of $E_d=80$ MeV, the bin size $\Delta k=0.48$ fm^{-1} seems to be already satisfactory since $|\hat{S}(L)|$ reaches con-

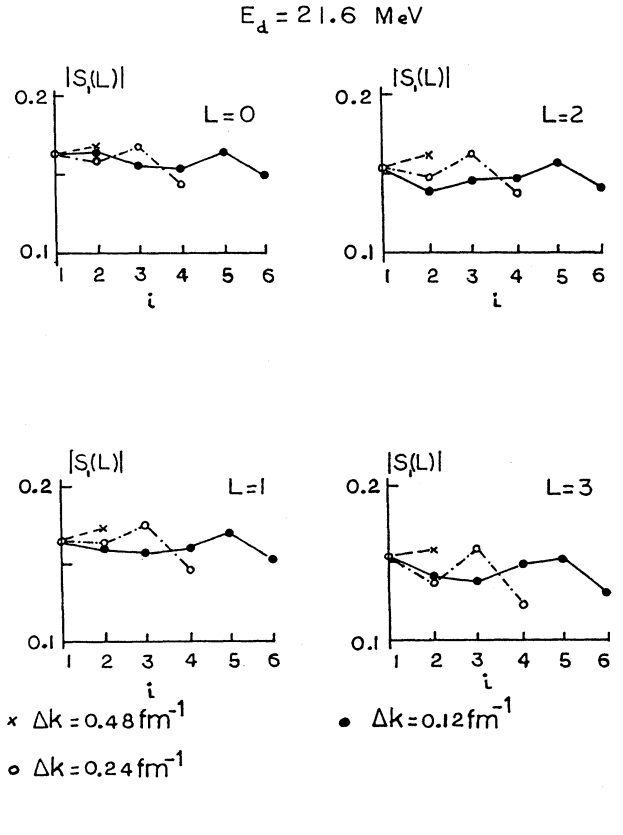

FIG. 12. Reflection coefficients $|S(L)|$ vs bin numbers i for bin sizes $\Delta k=0.48$ fm, 0.24 fm, 0.12 fm, and $E_d=21.6$ MeV. No coupling is denoted with $i=1$. The angular momenta L are indicated next to the curves.

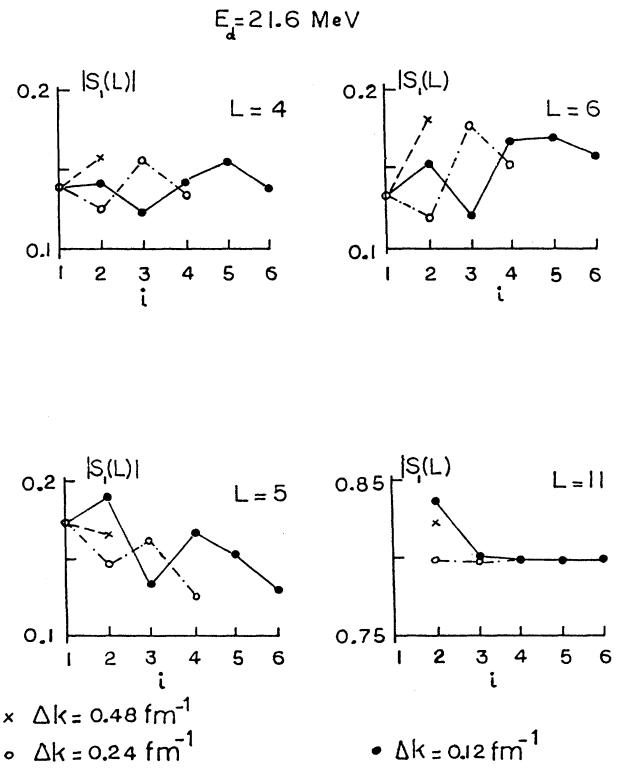

FIG. 13. Same as Fig. 12 for additional values of L.

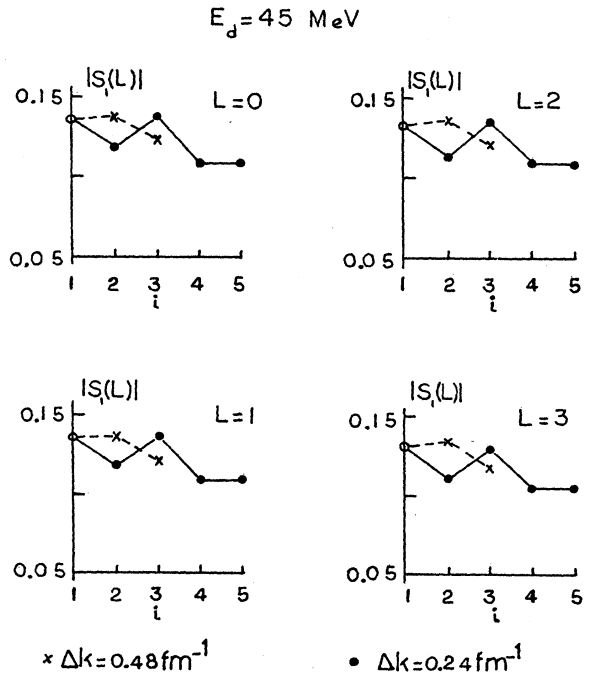

FIG. 14. Reflection coefficients $|S(L)|$ vs bin numbers i for bin sizes $\Delta k = 0.48$ fm, 0.24 fm, and $E_d = 45$ MeV.

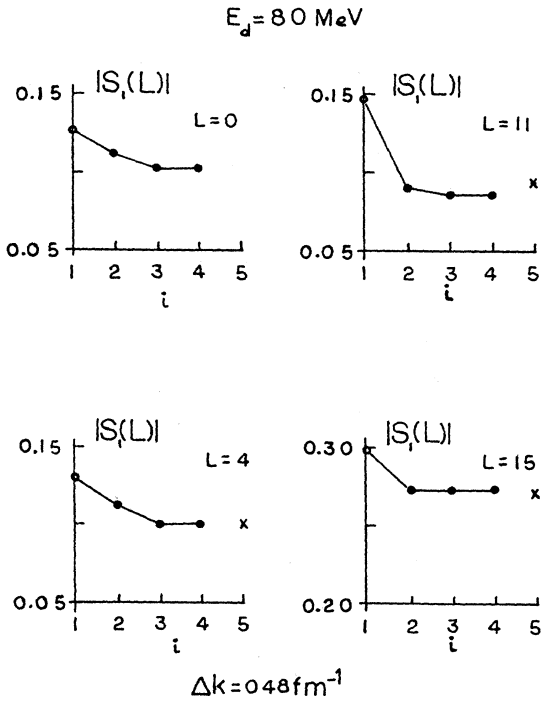

FIG. 16. Reflection coefficients $|S(L)|$ vs bin numbers i for bin size $\Delta k = 0.48$ fm^{-1} and $E_d = 80$ MeV.

vergence (see Fig. 16).

The comparison of the elastic S-matrix elements for the two methods of discretization will now be discussed. Figures 17 and 18 show the Argand diagrams of the converged values of the S-matrix elements at energies 21.6 and 45 MeV, respectively. In Fig. 17 solid circles designate the results of the k-bin calculations with $\Delta k = 0.12$ fm^{-1}. The crosses correspond to the results of the diagonalization procedure using the set of eigenfunctions $\Phi_n^{(12)}$ correspond to $\Delta k_n = 0.10$ fm^{-1}. Apart from $L = 8$, both calculations are in very good agreement. In the case of $E_d = 45$ MeV (Fig. 18), the points are even closer to each

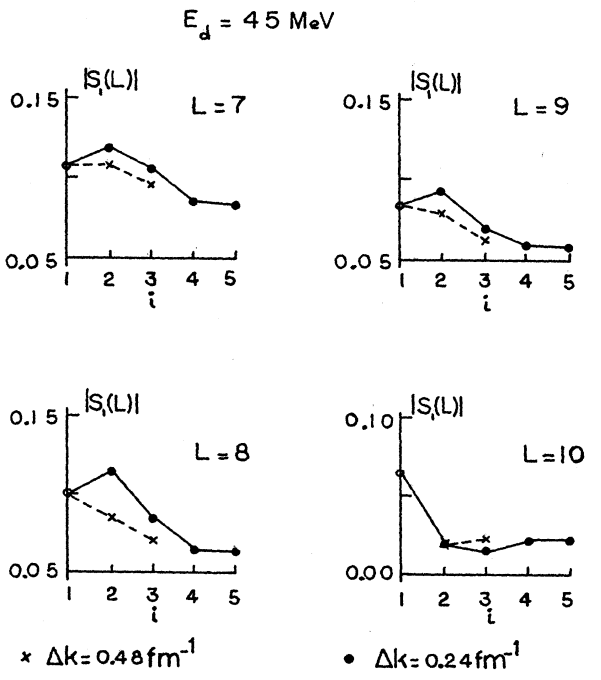

FIG. 15. Same as Fig. 14 for additional values of L.

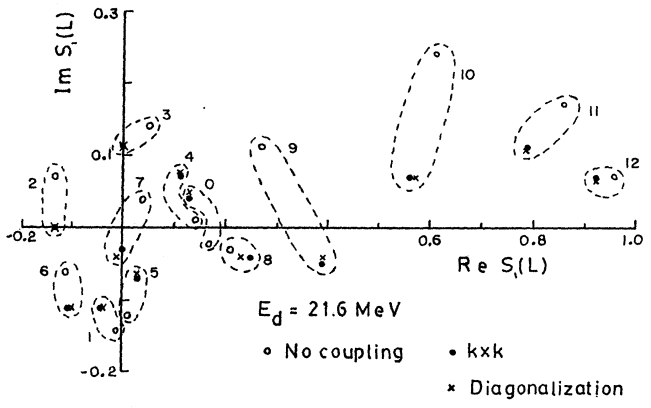

FIG. 17. Argand diagram showing the elastic scattering matrix elements. The crosses ($\times$) show the diagonalization results obtained with $N = 12$ and $r_0 = 20$ fm. The solid circles (●) represent the bin discretization results with $\Delta k = 0.12$ fm^{-1}. The incident energy is $E_d = 21.6$ MeV.

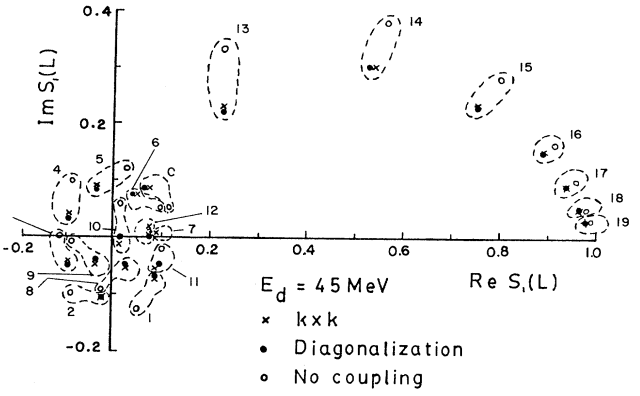

FIG. 18. Same as Fig. 17 for an incident energy of 45 MeV.

other than in the 21.6 MeV case, which seems to indicate that the agreement between the two methods of discretization become even better at high energies. In conclusion, the two methods of diagonalization give closely similar results for the elastic deuteron channel S- matrix elements, even though they differ slightly in the long-range part of the coupling potentials.

C. Sensitivity to the long-range part of the potentials

In a separate study[17] it was shown that changes of the long-range parts of the potentials in the channels coupled to the elastic one (both the diagonal potentials as well as the interchannel coupling potentials) should affect very little the elastic S-matrix elements. This conclusion is based on a cancellation which occurs in an integral involving Green's functions and the tails of the potentials in question. The cancellation takes place provided that (1) these changes occur at distances larger than the ranges of the elastic-to-inelastic coupling potentials $V_{1,n}(R)$ and (2) that for these long-range distances the irregular solution in the coupled channels (i.e., the channels other than the elastic one) are strongly oscillatory. Condition (2) is satisfied if the Wentzel-Kramers-Brillouin (WKB) approximation for the wave function in the coupled channels is valid in the region of space starting from distances less than the range of the $V_{1,n}$'s and extending to infinity. Thus it should not be valid for the high partial waves, whose turning points lie in the radial region previously mentioned. Condition (2) should also not be valid for the case when the energies in the coupled channels become so low that the corresponding wave numbers are larger than the distances over which the tails of the potentials in the coupled channels vary significantly.

Inspection of Figs. 4 and 5 shows that the range of the potentials in breakup space is significantly larger than the range of the bound-to-continuum transition potentials, and hence the conditions (1) and (2) previously stated are likely to be satisfied for the low partial waves, and also provided that the incident deuteron energy is high enough so that the energies in the important breakup channels are not too low.

The purpose of this section is to present a numerical

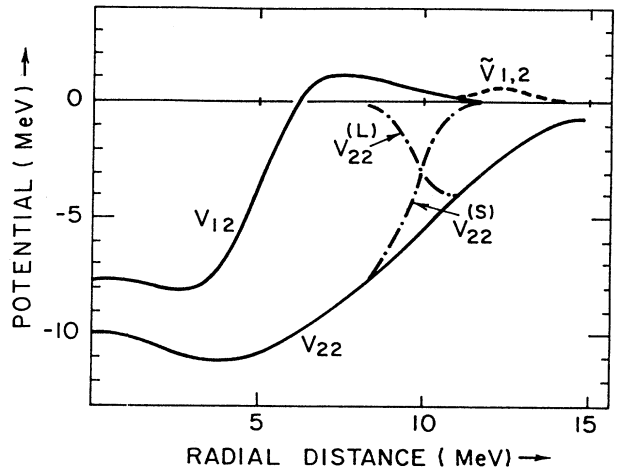

FIG. 19. Separation of $V_{2,2}$ into short (s) and long (l) ranged parts. The range of $V^{(l)}$ is chosen to be comparable to that of $V_{1,2}$. Dashed line illustrates the artificially extended part of $V_{1,2}$. Only the real parts are shown.

confirmation of the predictions of Ref. 17. The calculation consists in separating the potentials in the breakup space into short- and long-ranged components

$$V = V^{(l)} + V^{(s)} , \tag{3.2}$$

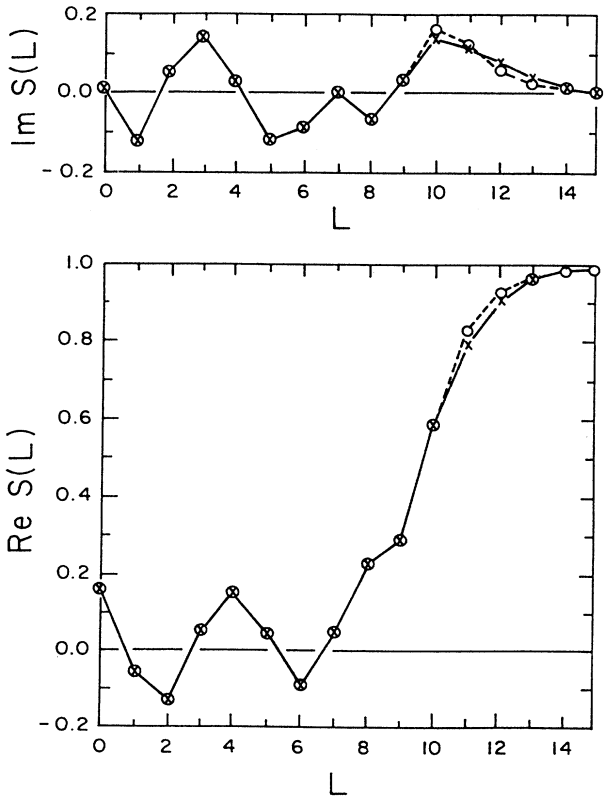

FIG. 20. The elastic scattering matrix elements $S(L)$ for the two channel case. The open circles ($\circ$) show the results for the case that the (l) and (s) parts of $V_{2,2}$ are both included. The crosses indicate the results when only the (s) part is included.

TABLE II. Center of mass channel energies.

Channel	Energy (MeV)	Channel	Energy (MeV)
1	20.88	4	12.87
2	17.96	5	8.63
3	15.99	6	3.29
		7	−3.16

and then ascertaining what effect the long-ranged parts have on the elastic scattering matrix elements. The short-ranged parts, $V^{(s)}_{n,n'}$ are chosen to have approximately the range of the $V_{1,n}$'s. This is accomplished by applying a smooth cutoff to the $V_{n,n'}$'s by means of the function $[1-\Theta(R)]$ which goes to zero for $R \ll R_{\rm cut}$ and goes to unity for $R \gg R_{\rm cut}$

$$V^{(s)}_{n,n'}(R)=V_{n,n'}(R)[1-\Theta(R)] ,$$
$$V^{(l)}_{n,n'}(R)=V_{n,n'}(R)[\Theta(R)] , \tag{3.3}$$

where

$$\Theta(R)=\tfrac{1}{2}\{1+\tanh[(R-R_{\rm cut})/a_{\rm cut}]\} . \tag{3.4}$$

In the application described below, $R_{\rm cut}$ and $a_{\rm cut}$ are given the values 10 fm and 0.8333 fm, respectively. In the numerical calculation the L^2 method of discretization is chosen, with the parameters r_0 and α having the values of 20 fm and 0.52 MeV fm^{-2}, respectively. The calculation is done for the case of 21.6 MeV deuterons incident on ^{58}Ni, and either the two channel or the seven channel cases are considered. Some of the potentials are illustrated in Figs. 4 and 5. The breakup energies and the corresponding channel energies are listed in Table II.

For the two channel case the (l) and (s) parts of the diagonal potential in the breakup channel (channel 2) is illustrated in Fig. 19. The corresponding effect on the elastic S-matrix element is shown in Fig. 20. One sees that the presence or absence of the relatively large bell-shaped potential tail $V^{(l)}_{2,2}$ has a rather minor effect on $S(L)$, the effect becoming larger for the large L values, as is to be expected from the theoretical argument.[16] Calculations have also been performed[9] in which the tail of the coupling potential $V_{1,2}$ is artificially increased by the amount $\tilde{V}_{1,2}$ (also illustrated in Fig. 19). The effect which the latter has is comparable to the effect which $V^{(L)}_{2,2}$ has, even though the former is much smaller in magnitude than the latter.

In the seven channel case a smooth cutoff of the long-ranged parts of the potentials in breakup space has a similar effect to that seen in the two channel case, only the changes in S already occur for smaller values of L. This result is consistent with the expectation of the discussion made above. The effects on S are illustrated in Fig. 21, in the form of an Argand diagram. A sharp cutoff was also performed by decreasing the value of the matching radius (beyond which all potentials other than the Coulomb potential are set to zero). The result is also shown in Fig. 21.

In conclusion, the numerical calculations confirm the expectation[17] that errors in the long-ranged parts of the potentials in breakup space do not significantly propagate into the elastic scattering matrix elements. Since the discretization mainly affects the long-ranged parts of these potentials, the result obtained in this section is responsible to a large extent for the success of the discretization methods analyzed in the present study.

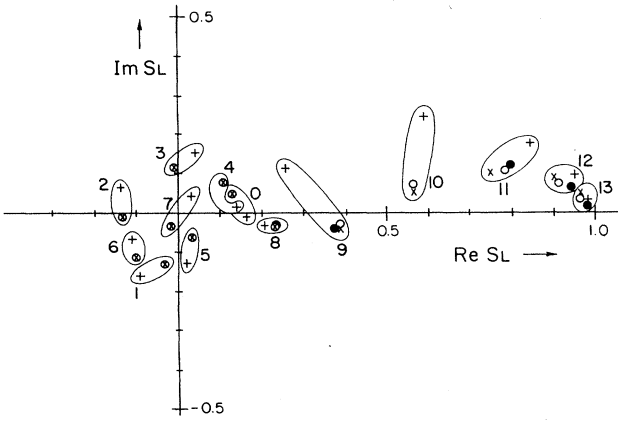

FIG. 21. Argand diagram of the elastic scattering matrix elements $S(L)$ for 21.6 MeV deuteron incident on ^{58}Ni. The (+) indicate the results without coupling to the breakup channels. All the other cases include coupling to six breakup channels, in the diagonalization procedure, as is described in the text. The solid circles (●) denote the case calculated in the presence of the complete ($L+S$) inelastic potentials, and the matching radius taken as 10 fm. The other two cases have the matching radius equal to 15 fm. The open circles (○) and crosses (×) denote, respectively, the results calculated with and without the long range parts of the inelastic potentials. When the solid and open circles coincide then only the open circles are shown. The results corresponding to the same orbital angular momentum L have been grouped together and the value of L is indicated for each group.

IV. SUMMARY AND CONCLUSIONS

We have used two discretization methods for the purpose of studying the effect of breakup on the elastic scattering matrix elements, $S^{(N)}_1$. These are the momentum bin averaging method and the L^2 diagonalization method. We have examined the convergence of $S^{(N)}_1$ with the number and density of discretization states and we found that the values of $S^{(N)}_1$ converge to the same result for either method. We also discovered that the rapidity of convergence is energy dependent. For incident deuteron energies below 20 MeV, high discretization state density or small bin size Δk (slow convergence) is needed to get stationary and reliable values. Above 45 MeV, converged values can be obtained with less dense sets of discretized states. This conclusion is based on numerical convergence studies carried out for ^{58}Ni as the target nucleus. But it is also expected to be true for nuclei such as Ca or Zn. The minimum size of breakup space needed to obtain the above convergence is 20 MeV of breakup ener-

gy, regardless of whether the breakup channels become closed or not. Inclusion of the breakup states with relative n-p angular momenta larger than zero, neglected in the present study, may require an increase in this minimum size of breakup space.

Another effect due to the changing of the discretization parameters is the modification of the long-range parts of the potentials which occur in the CDCC coupled equations. In a separate study[17] we found that the effect of such modifications upon the elastic S-matrix elements should be negligible provided that the changes occur in a region of space where the transition potentials between the elastic and inelastic channels are already small. Numerical calculations presented here confirm this expectation. This result may be the main reason for the good convergence, found in this study, of the elastic deuteron scattering elements with discretization parameters, especially for the higher incident deuteron energies.

Although the present report was limited to elastic scattering, it should also be mentioned that the deuteron breakup effect on transfer reaction cross sections such as (d,p) cross sections has been found important in the energy range up to $E_d = 80$ MeV. Different prescriptions[20–24] of including breakup effect into the stripping calculations have been studied and applied to various reactions. The results were indeed satisfactory. However, there still remain cases where there are serious disagreements with experiments.[25,26] It is fortunate that at these energies the methods of discretization investigated in the present work were found to be reliable.

ACKNOWLEDGMENTS

One of us (R.Y.R.) is very grateful to the Council for the International Exchange of Scholars for support received at the University of Connecticut under the Fulbright Program and to the Physics Department of the University of Connecticut for the kind hospitality. We both acknowledge the financial support received initially from the U.S. Department of Energy, Contract No. DE-AC-02-77-ERO-444. The computational facilities at the University of Connecticut proved to be invaluable for the calculations presented here, and are also much appreciated.

*Permanent address: Filiere Physique-Chimie, Ecole Normale Niveau 3, Universite d'Antananarivo, Antananarivo-101, Madagascar.

[1]M. Kawai and M. Kamimura, Prog. Theor. Phys. **59**, 674 (1978); M. Kawai and K. Takesako, *Proceedings of the 1978 INS International Symposium, Fukuoka, 1978* (Institute for Nuclear Study, University of Tokyo, Tokyo, Japan, 1979), pp. 719, 711, and 712.

[2]G. H. Rawitscher, Phys. Rev. C **9**, 2210 (1974); G. H. Rawitscher, Nucl. Phys. **A241**, 365 (1975); G. H. Rawitscher and S. N. Mukherjee, Ann. Phys. (N.Y.) **123**, 90 (1978); Nucl. Phys. **A342**, 90 (1980).

[3]J. P. Farrell Jr., C. M. Vincent, and N. Austern, Ann. Phys. (N.Y.) **96**, 333 (1976); N. Austern, C. M. Vincent, and J. P. Farrell, *ibid.* **114**, 93 (1978).

[4]M. Yahiro and M. Kamimura, Prog. Theor. Phys. **65**, 2046 (1981); Y. Sakuragi, M. Yahiro, and M. Kamimura, *ibid.* **65**, 2051 (1981).

[5]M. Yahiro, M. Nakano, Y. Iseri, and M. Kamimura, Prog. Theor. Phys. **59**, 674 (1978); **69**, 1467 (1982).

[6]B. Anders and A. Lindner, Nucl. Phys. **A296**, 770 (1978).

[7]J. C. Johnson and P. C. Tandy, Nucl. Phys. **C11**, 1152 (1974).

[8]Z. C. Kuruoglu and F. S. Levin, Phys. Rev. Lett. **48**, 879 (1982); Ann. Phys. (N.Y.) **163**, 120 (1985); S. K. Adhikari, Z. C. Kuruoglu, and F. S. Levin, *ibid.* **163**, 149 (1985).

[9]R. Y. Rasoanaivo, Ph.D. dissertation, University of Connecticut, 1982.

[10]N. Austern and M. Kawai, Prog. Theor. Phys. **80**, 694 (1988); T. Sawada and K. Thushima, *ibid.* **76**, 440 (1986); T. Sawada and K. Thushima, in *Fewbody Approaches to Nuclear Reactions in Tandem and Cyclotron Energy Regions*, edited by S. Oryu and T. Sawada (World Scientific, Singapore, 1987) p. 227; T. Sawada and K. Thushima, Prog. Theor. Phys. **79**, 1378 (1988).

[11]Y. Sakuragi, M. Yahiro, and M. Kamimura, Prog. Theor. Phys. **89**, 136 (1986).

[12]M. Kawai, Prog. Theor. Phys. Suppl. **89**, 11-31 (1986); M. Kamimura, M. Yahiro, Y. Iseri, Y. Sakuragi, H. Kameyama, and M. Kawai, *ibid.* **89**, 1 (1986).

[13]N. Austern, Y. Iseri, M. Kamimura, M. Kawai, G. Rawitscher, and M. Yahiro, Phys. Rep. **154**(3), 125 (1987).

[14]R. Rotenberg, Ann. Phys. (N.Y.) **19**, 262 (1962).

[15]V. Numerov, Observ. Astrophys. Centrale Russie **2**, 188 (1923).

[16]K. Smith, *The Calculation of Atomic Collision Process* (Wiley, New York, 1970).

[17]G. H. Rawitscher and R. Y. Rasoanaivo, Phys. Rev. C **27**, 1078 (1983).

[18]F. G. Perey, Phys. Rev. **131**, 745 (1963); F. G. Perey and B. Buck, Nucl. Phys. **32**, 353 (1962).

[19]F. D. Becchetti Jr. and G. W. Greenlees, Phys. Rev. **182**, 1190 (1969).

[20]R. C. Johnson and P. J. R. Soper, Phys. Rev. C **1**, 976 (1970).

[21]G. H. Rawitscher, Phys. Rev. C **11**, 1152 (1975).

[22]M. Kawai, M. Kamimura, and K. Takesako, Prog. Theor. Phys. **89**, 118–135 (1986).

[23]M. Iseri, Ph.D. thesis, Kyushu University, Japan, 1985.

[24]T. K. Roy and S. Mukherjee, J. Phys. G **13**, 1239 (1987).

[25]E. J. Stephenson *et al.*, Phys. Lett. B **171**, 358 (1986); Nucl. Phys., **A469**, 467 (1987); V. R. Cupps *et al.*, *ibid.* **A469**, 445 (1987).

[26]E. J. Stephenson, R. C. Johnson, J. A. Tostevin, Bull. Am. Phys. Soc. **33**, 1571 (1988); B. K. Park, A. D. Bacher, G. P. A. Berg, V. R. Cupps, D. A. Low, D. W. Miller, C. Olmer, A. K. Opper R. Sawafta, E. J. Stephenson, and S. W. Wissnik, *ibid.* **33**, 1582 (1988).